How to cite: *Angew. Chem. Int. Ed.* **2021**, *60*, 4470–4473
International Edition: doi.org/10.1002/anie.202012722
German Edition: doi.org/10.1002/ange.202012722

Nitride Zeolites

Synthesis of Nitride Zeolites in a Hot Isostatic Press

*Sebastian Wendl, Mirjam Zipkat, Philipp Strobel, Peter J. Schmidt, and Wolfgang Schnick**

Abstract: *The recently introduced nitridophosphate synthesis in a hot isostatic press (HIP) enabled simple access to large-scale product quantities starting from exclusively commercially available starting materials. Herein, we show that this method is suitable for the synthesis of highly condensed functional nitridophosphates, as well. Hence, the syntheses of the nitridophosphate zeolites $Ba_3P_5N_{10}X$ (X = Cl, Br) are presented as proof of concept for this innovative access. Furthermore, samples of unprecedented $Sr_3P_5N_{10}X$ (X = Cl, Br) were prepared and characterized to demonstrate the advantages of this synthetic approach over commonly used methods. Luminescence investigations on Eu^{2+}-doped samples of $AE_3P_5N_{10}X$ (AE = Sr, Ba; X = Cl, Br) were carried out and characteristics of observed emission bands are discussed.*

The versatile compound class of nitridophosphates has been researched in detail for more than 30 years.[1] The structural diversity of nitridophosphates can be derived from their close relationship to oxosilicates, as the element combination Si/O is isoelectronic with P/N, and similar with oxosilicates which are built up from SiO_4 tetrahedra, the PN_4 tetrahedron is the fundamental building unit in nitridophosphates. However, nitridophosphates can even feature edge-sharing tetrahedra due to the higher covalence (and lower polarity) of P–N bonds compared to Si–O in oxosilicates.[1,2] Additionally, the higher valence of nitrogen allows for higher degrees of condensation (i.e. atomic ratio κ of tetrahedra centers to tetrahedra vertices).[1,3] But despite numerous investigations, nitridophosphate synthesis has ever been challenging, as the most common starting material phosphorus(V) nitride (P_3N_5) is prone to thermal decomposition above 850 °C.[4] Therefore, high-pressure high-temperature methods (e.g. multianvil technique) have been employed for their synthesis, since elevated nitrogen pressure suppresses the thermally induced elimination of N_2 from P_3N_5.[1] This high-pressure strategy led to a large number of nitridophosphates with various incorporated electropositive elements.[5–9] However, sample quantities have intrinsically been limited by high-pressure techniques. Investigations on the associated optical and physical properties of nitridophosphates, such as ion conductivity or luminescence, have however quickly revealed the potential of this functional materials class.[5,10–12] In particular, the intriguing luminescence properties of nitridophosphates like $Ba_3P_5N_{10}X$:Eu^{2+} (X = Cl, Br, I) and AEP_8N_{14}:Eu^{2+} (AE = Ca, Sr, Ba) clearly underline the quest for a synthetic approach that can be transformed to a large batch scale.[3,11,13] Here, ambient and medium-pressure methods that have been used for the early syntheses of phosphorus nitrides and nitridophosphates come to mind.[14–23] However, only a limited number of such nitride compounds could be synthesized applying these techniques, as gentle conditions or tailored starting materials had to be used. This limitation has changed only recently, as improved high-temperature ammonothermal techniques and the use of red phosphorus as starting material enabled synthesis of diverse nitridophosphates.[24–27] However, ammonothermal syntheses of nitridophosphates may not be performed industrially due to its demanding handling and the stated goal for a large-scale access remained. Recently, we have reported on the successful synthesis of Ca_2PN_3 in a hot isostatic press (HIP) under nitrogen pressure, which thus appears as a promising innovative approach for nitridophosphate synthesis.[28] HIPs do not only provide large sample quantities, but also shorten reaction times and facilitate crystal growth under comparatively gentle reaction conditions. Moreover, we have demonstrated that red phosphorus can serve as a starting material in HIPs as well, simplifying nitridophosphate syntheses even more.[28]

Within the scope of this work, this approach is further developed to grant access to highly condensed nitridophosphates with a degree of condensation $\kappa = 1/2$. For this purpose, $Ba_3P_5N_{10}X$ (X = Cl, Br) were chosen as model compounds, because of their above-mentioned luminescence properties.[11,13] Furthermore, hitherto unknown compounds $Sr_3P_5N_{10}X$ (X = Cl, Br) were synthesized and investigated with regard to luminescence properties.

All alkaline earth nitridophosphate zeolites $AE_3P_5N_{10}X$ (AE = Ba, Sr; X = Cl, Br) were synthesized under nitrogen atmosphere in a HIP applying hot isostatic conditions (150 MPa N_2, 1000 °C, Figures S1 and S2). In an initial attempt, the title compounds were synthesized from specially prepared P_3N_5 and the respective alkaline earth azides and halides following Equation (1) (Table S1).

$$15\,AE(N_3)_2 + 3\,AEX_2 + 10\,P_3N_5 \rightarrow 6\,AE_3P_5N_{10}X + 40\,N_2 \quad (1)$$

Subsequently, all variants of $AE_3P_5N_{10}X$ (AE = Ba, Sr; X = Cl, Br) were prepared using commercial red phosphorus

[*] S. Wendl, M. Zipkat, Prof. Dr. W. Schnick
Department of Chemistry, University of Munich (LMU)
Butenandtstr. 5–13, 81377 München (Germany)
E-mail: wolfgang.schnick@uni-muenchen.de
Dr. P. Strobel, Dr. P. J. Schmidt
Lumileds Phosphor Center Aachen, Lumileds (Germany) GmbH
Philipsstr. 8, 52068 Aachen (Germany)
Supporting information and the ORCID identification number(s) for the author(s) of this article can be found under: https://doi.org/10.1002/anie.202012722.

© 2020 The Authors. Angewandte Chemie International Edition published by Wiley-VCH GmbH. This is an open access article under the terms of the Creative Commons Attribution Non-Commercial NoDerivs License, which permits use and distribution in any medium, provided the original work is properly cited, the use is non-commercial and no modifications or adaptations are made.

(P_{red}), replacing P_3N_5 as phosphorus source [Eq. (2), Table S1]. The reaction equation is balanced with P_4, since P_{red} is considered to transform into molecular/gaseous phosphorus at reaction conditions of 150 MPa and 1000 °C.[28]

$$10\,AE(N_3)_2 + 2\,AEX_2 + 5\,P_4 \rightarrow 4\,AE_3P_5N_{10}X + 10\,N_2 \qquad (2)$$

Subsequent oxidation into P^V is coupled to the disproportionation of azide ions into network-forming nitride anions and elemental nitrogen. Thereby, it is conceivable that activated P_4 is gradually oxidized and present as P^{III} in form of molecular "PN" after initial reaction with N_2. In a second oxidization step, halide-containing intermediates, such as $(P^VNCl_2)_3$, might be formed. $(PNCl_2)_3$ in turn serves as starting material for laboratory synthesis of P_3N_5 and may facilitate the in situ formation of the latter, leading to the desired zeolites $AE_3P_5N_{10}X$. An experimental evidence for this hypothesis by in situ measurements is still pending.

To investigate luminescence properties of $AE_3P_5N_{10}X$, Eu^{2+}-doped samples were prepared by adding 3 mol % $EuCl_2$ (with regard to alkaline earth ions) to the mixture of starting materials.

The undoped samples are yielded as colorless cube-like crystals, while sinter cakes of Eu^{2+}-doped products exhibit yellow (Ba compounds) to orange body colors (Sr compounds). All products have been washed with de-ionized water and are not sensitive towards air or moisture. SEM imaging of the products reveals the microcrystalline character of Ba compounds (edge length up to ≈3 μm, Figure 1). Sr compounds form slightly larger crystals with edge lengths up to 15–20 μm (Figure 1). Phase purity of $Ba_3P_5N_{10}X$ (X = Cl, Br) was confirmed by Rietveld refinements, using literature known structures as starting models.[11,13] Detailed information on the refinements is provided in the Supporting Information (Figures S3 and S4, Table S2).

The structures of $Sr_3P_5N_{10}X$ (X = Cl, Br) were elucidated from a single-crystal XRD measurement of $Sr_3P_5N_{10}Cl$. $Sr_3P_5N_{10}Br$ was refined using the Rietveld method and using the structure of $Sr_3P_5N_{10}Cl$ as starting model (Figure S5, Table S7). Both compounds crystallize homeotypically to the Ba compounds in the *JOZ* zeolite structure type (*Pnma*; Z = 8; $Sr_3P_5N_{10}Cl$: a = 12.240(3); b = 12.953(3); c = 13.427(3) Å; $Sr_3P_5N_{10}Br$: a = 12.297(1); b = 12.990(1); c = 13.458(1) Å.[29–31] The crystal structure of $Sr_3P_5N_{10}X$ is shown exemplarily for X = Cl in Figure 2. The as-refined crystallographic data is summarized in the Supporting Information (Tables S3–S5) and a more detailed description of the crystal structure is provided in literature.[11,13] Phase purity of $Sr_3P_5N_{10}Cl$ has been confirmed by Rietveld refinement (Figure S6, Table S7). In contrast to the Ba compounds, $Sr_3P_5N_{10}X$ (X = Cl, Br) show split positions of the Sr5 site. Although the split position is not present in the Ba compounds the corresponding Ba5 site in $Ba_3P_5N_{10}X$, however, shows the most elongated ellipsoids and Ba–X distances (Figure S7).[11,13] This observation can be explained by the significantly smaller space filling of Sr^{2+} compared to Ba^{2+} and the associated increasing displacement of ions.[32,33] Moreover, owing to the larger radius of Br^-, the distance between the split position is reduced in $Sr_3P_5N_{10}Br$ (Figure S8).

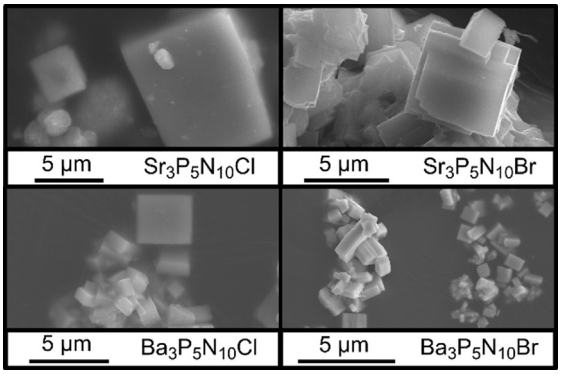

Figure 1. SEM images of obtained $AE_3P_5N_{10}X$ samples (AE = Sr, Ba; X = Cl, Br) containing single crystals.

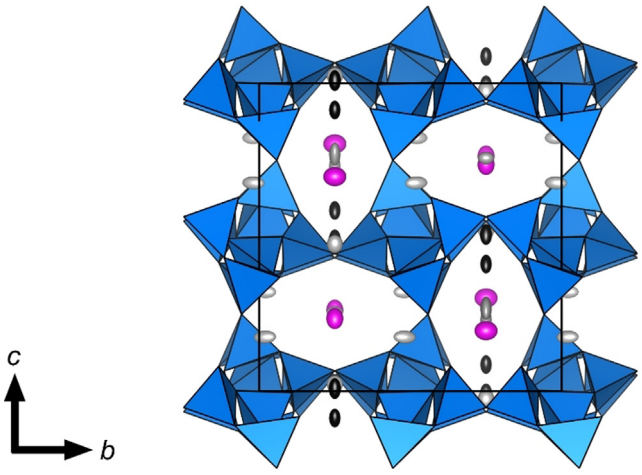

Figure 2. Projection of the crystal structure of $Sr_3P_5N_{10}Cl$ along [100]: PN_4 tetrahedra blue, Cl atoms pink, Sr1–Sr4 atoms gray, split position of Sr5 black. All atoms are displayed with 95 % probability.[29]

These observations may explain the reason for $Sr_3P_5N_{10}X$ (X = Cl, Br) being exclusively accessible at medium-pressure conditions, as the pressure has to be well balanced. Although increased pressure is necessary to prevent thermal decomposition, it must not be chosen too high for $Sr_3P_5N_{10}X$ syntheses to prevent collapsing of the large cages, considering the reduced space filling of the Sr^{2+} ions. In line with this hypothesis, the Ba compounds are rather difficult to access at ambient pressure, as well, and phase pure samples have only been obtained at 1–5 GPa, thus far.[11,13]

The interatomic P–N distances and N-P-N angles of $Sr_3P_5N_{10}X$ (X = Cl, Br) are in very good agreement with values reported for other nitridophosphates (Table S9).[3,11–13] In line with previous refinements, the observed AE–N/X distances differ significantly depending on the coordination number of the alkaline earth metal ion (Figure S8). A detailed list of the interatomic AE–N/X distances is provided in literature for $Ba_3P_5N_{10}X$ and in the Supporting Information for $Sr_3P_5N_{10}X$ (Table S8).[11,13]

The chemical compositions of the title compounds were confirmed by energy dispersive X-ray spectroscopy (EDX),

 © 2020 The Authors. Angewandte Chemie International Edition published by Wiley-VCH GmbH

with details provided in the Supporting Information (Tables S10).

Eu^{2+}-doped samples of $Ba_3P_5N_{10}X$ (X = Cl, Br) have already been discussed as promising phosphor materials, but any industrial application had been ruled out, owing to limited sample volumes.[11,13] With the innovative approach that is presented herein, large-volume samples become accessible. Additionally, hitherto unknown $Sr_3P_5N_{10}X:Eu^{2+}$ (X = Cl, Br) is introduced as new luminescent material.

Excitation with UV to blue light (λ_{exc} = 420 nm) induces natural-white ($Ba_3P_5N_{10}Br:Eu^{2+}$), orange ($Ba_3P_5N_{10}Cl:Eu^{2+}$), and deep-red emission ($Sr_3P_5N_{10}X:Eu^{2+}$), which features two emission maxima for each compound (Figures 3 and S9–13).

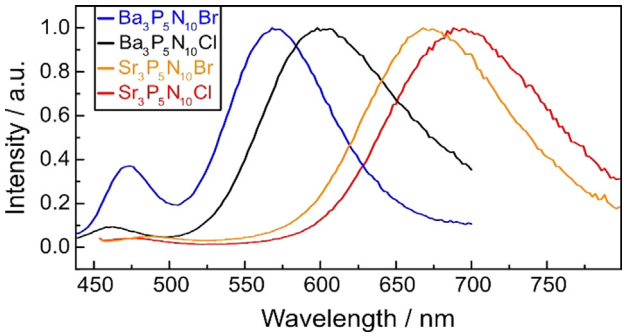

Figure 3. Measured emission spectra of $AE_3P_5N_{10}X:Eu^{2+}$ (AE = Sr, Ba; X = Cl, Br) at room temperature with a nominal doping level of 3 mol% Eu^{2+} referred to AE^{2+}.

The two emission maxima likely correspond to the different Eu^{2+} coordination spheres that are provided by the host lattice. The sites $AE1$, $AE4$, and $AE5$ are coordinated by eight N and two X ions (CN = 10) and thus, feature rather elongated AE–X and AE–N distances, causing a weak crystal field (Figure S8, Table S8). Therefore, the higher energetic emission bands can be assigned to Eu^{2+} ions occupying these sites according to the parity-allowed transition $4f^7 \rightarrow 4f^65d^1$. Consequently, the second emission band is assigned to Eu^{2+} ions located on AE sites with lower coordination number ($AE2$, $AE3$: CN = 8, six N and two X ions), which feature shorter AE–X and AE–N distances and thus a strong crystal field (Figure S8, Table S8). A detailed illustration of the emission and excitation spectra for each element combination AE-X is provided in the Supporting Information (Figures S10–S13).

When comparing the emission spectra, two trends are particularly striking. First, emission bands of $AE_3P_5N_{10}Cl$ and $AE_3P_5N_{10}Br$ are shifted comparing AE = Ba and AE = Sr. This effect is attributable to the different AE radii and the associated AE–N/X and Eu^{2+}–N/X distances, leading to an increased crystal field splitting for Eu^{2+} on the Sr site and a red-shift in emission. The second trend describes the influence of the halide ions on the position of the emission maxima. While the higher energetic bands are shifted red with increasing size of X, lower energetic bands are shifted blue. A detailed discussion of these observations is provided in the Supporting Information.

Furthermore, measurements of the internal quantum efficiency have been carried out for non-optimized powder samples of the title compounds. The IQE of $Sr_3P_5N_{10}X:Eu^{2+}$ was determined to 29% (X = Cl) and 32% (X = Br). Measurements on $Ba_3P_5N_{10}X:Eu^{2+}$ yield quantum efficiency of 12% each, which shows potential for improvement of the investigated samples, as values of > 60% have been reported for $Ba_3P_5N_{10}X:Eu^{2+}$ (X = Cl, Br; 2 mol% Eu^{2+} referred to Ba^{2+}), previously.[11,13] The luminescence characteristics of the title compounds are summarized in Table S11.

Recapping, we have extended the possibilities of nitridophosphate syntheses by hot isostatic pressing. Prior to this work, this approach has been limited to preparation of lowly condensed $Ca_2PN_3:Eu^{2+}$. In this work, we have succeeded in synthesizing highly condensed nitridophosphates $AE_3P_5N_{10}X$ (AE = Sr, Ba; X = Cl, Br), increasing the maximum degree of condensation reachable for nitridophosphates by HIP synthesis to 1/2. It is particularly noteworthy that the used conditions allow for the synthesis of $Sr_3P_5N_{10}X$, which was not accessible by conventional methods, so far. Presumably, in this case only medium-pressure methods, such as hot isostatic pressing, enable pressure balancing in a way that the synthesis is possible at all. The pressure should be high enough to prevent thermal decomposition, but not too high, otherwise large cages collapse due to lower space filling of Sr^{2+}.

The presented results suggest that the pressure range generally applied under HP/HT conditions may exceed the actually required synthesis pressure for nitridophosphates by far. Since the minimum pressure to suppress thermal decomposition is not known, numerous published and some novel nitridophosphates are already accessible under medium-pressure conditions. Consequently, future investigations may focus on synthesis of $Ca_3P_5N_{10}X$, other P/N based zeolites (e.g. *NPO* or *NPT*), and even higher condensed nitridophosphates (e.g. AEP_8N_{14}). In particular, the successful activation of red phosphorus as starting material could contribute to a considerable acceleration of these investigations. It should also be examined whether other starting materials, such as nitrides, can be replaced by precursors, like metals or alloys. The fact that N_2 can serve as necessary redox partner has already been shown in the synthesis of Ca_2PN_3.[28] These significant simplifications in synthesis, the wide range of achievable degrees of condensation and the large sample volumes may allow that nitridophosphates could find their way into industrial application as phosphor materials.

Acknowledgements

The authors thank Dr. Peter Mayer (Department of Chemistry at LMU) for the collection of single-crystal data, Volker Weiler (Lumileds Phosphor Center Aachen) for luminescence measurements, Lisa Gamperl for EDX and SEM measurements and Tobias Giftthaler (all Department of Chemistry) for support in practical work. Open access funding enabled and organized by Projekt DEAL.

 © 2020 The Authors. Angewandte Chemie International Edition published by Wiley-VCH GmbH

Conflict of interest

The authors declare no conflict of interest.

Keywords: hot isostatic press · luminescence · medium-pressure · nitridophosphates · zeolites

[1] S. D. Kloß, W. Schnick, *Angew. Chem. Int. Ed.* **2019**, *58*, 7933 – 7944; *Angew. Chem.* **2019**, *131*, 8015 – 8027.

[2] S. Horstmann, E. Irran, W. Schnick, *Angew. Chem. Int. Ed. Engl.* **1997**, *36*, 1992 – 1994; *Angew. Chem.* **1997**, *109*, 2085 – 2087.

[3] S. Wendl, L. Eisenburger, P. Strobel, D. Günther, J. P. Wright, P. J. Schmidt, O. Oeckler, W. Schnick, *Chem. Eur. J.* **2020**, *26*, 7292 – 7298.

[4] W. Schnick, *Angew. Chem. Int. Ed. Engl.* **1993**, *32*, 806 – 818; *Angew. Chem.* **1993**, *105*, 846 – 858.

[5] E.-M. Bertschler, C. Dietrich, J. Janek, W. Schnick, *Chem. Eur. J.* **2017**, *23*, 2185 – 2191.

[6] F. W. Karau, W. Schnick, *J. Solid State Chem.* **2005**, *178*, 135 – 141.

[7] S. D. Kloß, W. Schnick, *Angew. Chem. Int. Ed.* **2015**, *54*, 11250 – 11253; *Angew. Chem.* **2015**, *127*, 11402 – 11405.

[8] F. J. Pucher, S. R. Römer, F. W. Karau, W. Schnick, *Chem. Eur. J.* **2010**, *16*, 7208 – 7214.

[9] S. Vogel, A. T. Buda, W. Schnick, *Angew. Chem. Int. Ed.* **2018**, *57*, 13202 – 13205; *Angew. Chem.* **2018**, *130*, 13386 – 13389.

[10] E.-M. Bertschler, C. Dietrich, T. Leichtweiß, J. Janek, W. Schnick, *Chem. Eur. J.* **2018**, *24*, 196 – 205.

[11] A. Marchuk, S. Wendl, N. Imamovic, F. Tambornino, D. Wiechert, P. J. Schmidt, W. Schnick, *Chem. Mater.* **2015**, *27*, 6432 – 6441.

[12] F. J. Pucher, A. Marchuk, P. J. Schmidt, D. Wiechert, W. Schnick, *Chem. Eur. J.* **2015**, *21*, 6443 – 6448.

[13] A. Marchuk, W. Schnick, *Angew. Chem. Int. Ed.* **2015**, *54*, 2383 – 2387; *Angew. Chem.* **2015**, *127*, 2413 – 2417.

[14] F. Golinski, H. Jacobs, *Z. Anorg. Allg. Chem.* **1995**, *621*, 29 – 33.

[15] H. Jacobs, F. Golinski, *Z. Anorg. Allg. Chem.* **1994**, *620*, 531 – 534.

[16] H. Jacobs, R. Nymwegen, *Z. Anorg. Allg. Chem.* **1997**, *623*, 429 – 433.

[17] H. Jacobs, R. Nymwegen, S. Doyle, T. Wroblewski, W. Kockelmann, *Z. Anorg. Allg. Chem.* **1997**, *623*, 1467 – 1474.

[18] H. Jacobs, S. Pollok, F. Golinski, *Z. Anorg. Allg. Chem.* **1994**, *620*, 1213 – 1218.

[19] W. Schnick, U. Berger, *Angew. Chem. Int. Ed. Engl.* **1991**, *30*, 830 – 831; *Angew. Chem.* **1991**, *103*, 857 – 858.

[20] W. Schnick, J. Lücke, *Z. Anorg. Allg. Chem.* **1990**, *588*, 19 – 25.

[21] W. Schnick, J. Lücke, *Z. Anorg. Allg. Chem.* **1992**, *610*, 121 – 126.

[22] W. Schnick, J. Lücke, *Angew. Chem. Int. Ed. Engl.* **1992**, *31*, 213 – 215; *Angew. Chem.* **1992**, *104*, 208 – 209.

[23] W. Schnick, V. Schultz-Coulon, *Angew. Chem. Int. Ed. Engl.* **1993**, *32*, 280 – 281; *Angew. Chem.* **1993**, *105*, 308 – 309.

[24] M. Mallmann, C. Maak, R. Niklaus, W. Schnick, *Chem. Eur. J.* **2018**, *24*, 13963 – 13970.

[25] M. Mallmann, S. Wendl, W. Schnick, *Chem. Eur. J.* **2020**, *26*, 2067 – 2072.

[26] M. Mallmann, S. Wendl, P. Strobel, P. J. Schmidt, W. Schnick, *Chem. Eur. J.* **2020**, *26*, 6257 – 6263.

[27] S. Wendl, M. Mallmann, P. Strobel, P. J. Schmidt, W. Schnick, *Eur. J. Inorg. Chem.* **2020**, 841 – 846.

[28] S. Wendl, S. Mardazad, P. Strobel, P. J. Schmidt, W. Schnick, *Angew. Chem. Int. Ed.* **2020**, *59*, 18240 – 18243; *Angew. Chem.* **2020**, *132*, 18397 – 18400.

[29] Crystal data of $Sr_3P_5N_{10}X$ (orthorhombic, *Pnma* (no. 62)); X = Cl: $M = 593.26\ \mathrm{g\ mol^{-1}}$, $a = 12.241(2)$, $b = 12.953(3)$ and $c = 13.427(3)$ Å, $V = 2128.9(8)$ Å^3, $Z = 8$, $\rho = 3.702\ \mathrm{g\,cm^{-3}}$, $\mu = 15.980\ \mathrm{mm^{-1}}$, Mo-$K_\alpha$ ($\lambda = 0.71073$ Å, Bruker D8 Venture), $T = 293$ K, 33 698 observed reflections, 3522 independent reflections, 116 parameters, $R_{int} = 0.036$, $R_\sigma = 0.072$, $R1 = 0.034$, $wR2 = 0.069$, $GoF = 1.065$, residual electron density 3.360, $-1.277\ \mathrm{e\,Å^{-3}}$; X = Br: $M = 637.70\ \mathrm{g\,mol^{-1}}$, orthorhombic, *Pnma* (no. 62), $a = 12.2970(2)$, $b = 12.9896(2)$ and $c = 13.4585(2)$ Å, $V = 2149.76(5)$ Å^3, $Z = 8$, $\rho = 3.942\ \mathrm{g\,cm^{-3}}$, $\mu = 30.520\ \mathrm{mm^{-1}}$, Cu-$K_{\alpha 1}$ ($\lambda = 1.5406$ Å, Stoe StadiP), $T = 293$ K, 993 observed reflections, 101 parameters, $R_p = 0.035$, $R_{wp} = 0.046$, $R_{exp} = 0.020$, $R_{Bragg} = 0.022$, $GoF = 2.257$. Deposition Numbers 2011982 (for Cl) and 2012398 (for Br) contain the supplementary crystallographic data for this paper. These data are provided free of charge by the joint Cambridge Crystallographic Data Centre and Fachinformationszentrum Karlsruhe Access Structures service www.ccdc.cam.ac.uk/structures.

[30] C. Baerlocher, L. B. McCusker, *Database of Zeolite Structures:* http://www.iza-structure.org/databases/, accessed June **2020**.

[31] J. A. Armstrong, M. T. Weller, *J. Am. Chem. Soc.* **2010**, *132*, 15679 – 15686.

[32] W. H. Baur, *Crystallogr. Rev.* **1987**, *1*, 59 – 83.

[33] R. Shannon, *Acta Crystallogr. Sect. A* **1976**, *32*, 751 – 767.

Manuscript received: September 18, 2020
Accepted manuscript online: November 17, 2020
Version of record online: December 23, 2020

 © 2020 The Authors. Angewandte Chemie International Edition published by Wiley-VCH GmbH